Hyphenation of affinity capillary electrophoresis with mass spectrometry for the study of ligand-protein interactions: *n*-methylmorpholine acetate buffer and polydopamine-based coating as key assets

Clara Davoine, Marianne Fillet*

Laboratory for the Analysis of Medicines (LAM), Department of Pharmacy, CIRM, University of Liege, Avenue Hippocrate 15, B36 Tour 4 +3, 4000 Liège, Belgium.

ABSTRACT: The direct and precise assessment of ligand-protein interactions under near-physiological conditions is the core of drug discovery. In this context, affinity capillary electrophoresis (ACE) has become an emerging and reliable approach. The hyphenation of ACE with mass spectrometry (MS) is even more powerful than the classical ACE-UV methodology. It reduces compound identification errors and increases throughput by facilitating the analysis of mixtures. However, buffers and capillary coatings compatible with mass spectrometry and operating under physiological conditions are very limited. In this paper, *n*-methylmorpholine acetate buffer and polydopamine-based coating were highlighted as major assets for CE-MS studies involving native proteins. Thanks to its protein desorption property, *n*-methylmorpholine improved the peak shape of proteins during CE analysis at physiological pH. The polydopamine-based neutral coating developed in this study is simple to prepare and demonstrated high stability at pH 7.4, enabling its use with MS detector. The combination of these two key elements enabled us to successfully convert our ACE-UV method for coagulation factor XIIa into an ACE-MS approach operating at physiological pH. This study extends the scope of ACE for medicinal chemistry projects.

Drug discovery projects aim to create a new chemical entity that binds strongly to the target protein and affects its disease-associated function.[1] This process is complex and expensive.[2] Its first step is to screen a library of ligands and select hit compounds that reach a threshold value.[1,3] The hit compounds undergo a first round of chemical optimization to obtain lead compounds, which are molecules that have demonstrated therapeutic potential.[2,3] The second step consists in optimizing the lead compounds into a drug candidate.[1,3] During the drug discovery phase, this last step is the most significant cost driver of a new medicine.[2,4] Indeed, performing an optimization of poor-quality leads will result in a longer lead optimization program and a clinical phase with higher failing rate. Therefore, high-quality leads can boost productivity.[2] To obtain high-quality leads, the main requirements are: (1) a well-identified, highly-pure chemical library, (2) accurate affinity determination, and (3) validation of target engagement.[1,2,5] Target engagement is confirmed when the molecule is shown to bind directly to the target protein.[5] Target engagement is often verified by native MS, SPR, NMR, or microscale thermophoresis (MST).[2,5] However, each has its shortcomings. With native MS, determination of affinity constants in the gas phase is less reliable, as the absence of water molecules can affect molecular interactions.[6] SPR and MST require immobilized and fluorescently-labeled proteins, respectively. The functional integrity of the modified target must therefore be confirmed.[7] As for NMR, its use is limited by the cost of the instrument and the high protein consumption.[5,7]

In this context, affinity capillary electrophoresis (ACE) is emerging as a reliable approach for validating target engagement and accurately determining dissociation constants (K_D).[7–10] The general principle of ACE is an alteration in the electrophoretic mobility of the analyte due to its interaction with the target.[11] There are several experimental configurations; but for drug discovery, the most useful is partial-filling ACE. Indeed, ACE involves a low consumption of unmodified target, can evaluate a wide range of interaction strengths in near-physiological medium, and possesses a separative character that enables the evaluation of impure samples.[7,8,12] Coupling ACE with mass spectrometry (ACE-MS) is a powerful combination for drug discovery. It helps characterize analytes (by reducing compound identification errors) and facilitates affinity analysis of mixtures (by increasing throughput).[6,13–17] However, detection by MS also imposes limits on buffer composition and capillary coating. The buffer must be MS-compatible, and the capillary coating must be permanent to prevent polymer leakage into the MS instrument.

One of the most common, neutral, permanent coatings used in CE-MS is linear polyacrylamide (LPA).[18] However, the covalent attachment of LPA to the silica surface is achieved by silylation, leading to Si-O bonds. These siloxane linkages are unstable at alkaline pH. Damage has already been observed at pH above 4.6[19], generating polymer leakages. LPA can be also be bonded to silica through Si-C linkages, which are stable at alkaline pH, but this requires the use of Grignard reagent[19], a dangerous chemical. Among the emerging alternative strategies for polymer immobilization inside capillaries, polydopamine (PDA) demonstrated an unique set of characteristics: one of the simplest preparation process, stability between pH 3 and 11 similar to covalent coatings on many material surfaces, high hydrophilicity, and chemical reactivity with thiol and primary amine groups under mild alkaline conditions for further functionalization.[20–22] PDA is a self-adherent polymer that is obtained by dissolving dopamine in a mild alkaline aqueous solution (generally at pH 8.5).[23] After PDA deposition, a secondary coating can be grafted on to achieve the desired surface properties. In addition to this conventional two-step approach, PDA deposition and surface tethering can also be carried out simultaneously. This one-pot method offers a simpler procedure, and

can lead to a higher density of molecular immobilizations.[21] As far as we know, the only ACE assay that utilizes the properties of PDA is a CE-UV frontal analysis of bovine serum albumin-acetaminophen interaction in a Tris-HCl buffer at pH 7.4.[24]

The ACE-MS conditions reported in the literature to date are not performed at physiological pH (7.4)[6,13–17], which compromises their value in the context of drug discovery. Volatile buffer systems for pH 7.4 are rare. High buffering capacity at this pH is achieved using ammonium bicarbonate, which is unstable over time and creates bubbles in the ESI source due to CO_2 outgassing.[25] As a more stable alternative, we investigated *n*-methylmorpholine (NMM), a volatile base with a pKa of 7.4 at 25°C[26]. To our knowledge, only two research articles analyzing acidic proteins by CE-MS reported the use of NMM as a buffer component for MS applications involving proteins.[27,28] As far as we know, the NMM-acetate buffer system has never before been used for ACE applications. Consequently, we studied its effect on CE analysis of small molecules and proteins using bare-fused silica capillary. Then, we optimized an easy-to-make, permanent, neutral coating using PDA grafted with a commercial amino-terminated neutral polymer. We also evaluated the impact of the oxidizing agent, the addition of an endcapping step, and storage conditions. Finally, the NMM-acetate buffer (pH 7.4) and our best PDA-based coating were used to determine the K_D of *p*-aminobenzamidine (PABZM) with coagulation factor XIIa (FXIIa) by ACE-MS.

EXPERIMENTAL SECTION

Materials

Acebutolol hydrochloride, avidin from egg white, betaxolol hydrochloride, bovine serum albumin (BSA) lyophilized powder, celiprolol hydrochloride, dopamine hydrochloride, flurbiprofen, ketorolac trometamol, labetalol hydrochloride, α-lactalbumin from bovine milk (type I), L-lysine, lysozyme from chicken egg white, 4-methylmorpholine (NMM, purity ≥ 99.5%), metoprolol tartrate, oxprenolol hydrochloride, niflumic acid, poly(N-isopropylacrylamide) (PIPAAm) amine terminated (average Mn 5,500), prilocaine, ribonuclease A from bovine pancreas, sotalol hydrochloride, and sulindac were purchased from Merck (Darmstadt, Germany). Para-aminobenzamidine dihydrochloride (PABZM) was sourced from Acros Organics (Fair Lawn, NJ). Acetylsalicylic acid, diclofenac sodium salt, ibuprofen, and salicylic acid were acquired from Fagron (Nazareth, Belgium). Human plasma β-factor XIIa (FXIIa) in solution at 1.15 mg/mL was purchased from Molecular Innovations (Novi, MI). CinnoRA® (adalimumab in solution at 50 mg/mL) was gifted by a partner. The reel of flexible fused silica capillary (75 µm i.d.) was provided by Polymicro Technologies, Inc. (Phoenix, AZ). The Tris-Hepes buffer was composed of 10 mM Trizma® hydrochloride (Tris), 10 mM 4-(2-hydroxyethyl)piperazine-1-ethanesulfonic acid (Hepes), 100 mM NaCl, adjusted at pH 7.4 with HCl. The NMM-acetate buffers were made by dissolving NMM in water at the desired concentration (150 mM, 300 mM, or 500 mM) and then adjusting the pH at 7.4 with acetic acid.

Physiochemical properties of the studied small molecules and proteins

The physicochemical properties of the small molecules were computed by MarvinSketch 19.27 (ChemAxon Ltd., Budapest, Hungary). The distribution coefficient (LogD) was calculated at pH 7.4 with an electrolyte concentration of 0.15 M NaCl. Solvent-accessible surface areas were computed at pH 7.4 using a solvent radius of 1.4 Å (approximated radius of a water molecule). All computed properties are available in Supplementary Materials (SM1—Small molecules' computed properties). The electrophoretic mobility of L-lysine without EOF in 150 mM NMM BGE was computed by PeakMaster version 6.0f8.[29]

The isoelectric point (pI) and the molecular weight (MW) of the proteins were found in the literature (lysozyme[30], ribonuclease A[30], avidin[31], α-lactalbumin[30], BSA[32], adalimumab[33]). The total charge of the proteins at pH 7.4 were determined by summing the charges of the exposed ionizable amino acids. Solvent-exposed ionizable amino acids were computed by Protein-sol pKa.[34] The different solvent-accessible areas (ASA) were calculated by the following procedure: (1) PDB files of the biological protein assembly cured of ligand and water molecules were obtained (lysozyme: 2LZT, ribonuclease A: 2E3W, avidin: 5IRU, α-lactalbumin: 1F6S, BSA: 4F5S, adalimumab: 3WD5-1HZH homology model[35]); (2) ASA of each atom was computed by GetArea 1.0 beta[36] with a probe radius of 10.0 Å (to exclude the surface of cavities inaccessible to solid interfaces[37]); (3) the potential field value and ratio of non-polar/polar were obtained for each atom thanks to the protein-sol patches software[38]; (4) the positive and negative ASA were calculated by summing the atomic surfaces of atoms having a potential field value ≥ 0 mV (ASA_+) and < 0 mV (ASA_-); (5) the hydrophobic and polar ASA were determined by summing the atomic surfaces of atoms possessing a ratio of non-polar/polar ≥ 1.45 (ASA_H) and < 1.45 (ASA_P). All computed properties are available in Supplementary Materials (SM2, proteins' properties).

PDA-coating procedures

All bare-fused silica capillaries (70 cm in total length) were pretreated by consecutively flushing methanol (67 min), 0.1 M HCl (67 min), water (11 min), 1.0 M NaOH (67 min), water (17 min), acetone (17 min), and air (67 min). In the layer-by-layer approach, the pretreated capillary was filled with 6 mg/mL dopamine hydrochloride in 10 mM Tris-HCl solution (pH 8.5). The capillary was sealed on both ends and incubated in a GC oven (Hewlett Packard Agilent HP 6890/G1530A Series GC System, Waldbronn, Germany) at 30°C for 20 h. The PDA deposition was repeated 0 or 1 times to obtain 1 or 2 layers of PDA on silica, respectively. Then, the capillary was rinsed with water (5 min) and helium stream (1 h, 30°C). PDA was grafted by injecting a solution of 25 mg/mL PIPAAm-NH_2 in 10 mM Tris-HCl solution (pH 8.5) and incubating the sealed capillary in the GC oven at 30°C for 30 h. The capillary was rinsed with water (5 min) and helium stream (15 min, 30°C). In the one-pot approach, the pretreated capillary was filled with a solution of 6 mg/mL dopamine hydrochloride and 25 mg/mL PIPAAm-NH_2 in 50 mM Tris-HCl (pH 8.5). The sealed capillary was then incubated in the GC oven at 30°C for 20 h and rinsed with water (5 min) and helium stream (1 h, 30°C). In the case of PDA deposition with oxidizing agent, these molecules were added in the dopamine solution before filling the capillary. In the case of endcapped coatings, the following step was added: the coated capillaries were filled with 100 mM Tris-HCl pH 8.5 (for Tris endcapping), 500 mM glycinamide hydrochloride adjusted at pH 8.5 with 1.0 M KOH (for glycinamide endcapping), 100 mM

thioglycerol in 50 mM Tris-HCl pH 8.5 (for thioglycerol endcapping), or 10 mg/mL BSA in 50 mM Tris-HCl pH 7.4 (for BSA endcapping). Then, they were incubated at 30°C for 72 h and rinsed with water (5 min) and helium stream (3 h, 30°C). Finally, the capillaries were cut to the desired length.

Capillary electrophoresis

CE-UV experiments were carried out on an Agilent 7100 capillary electrophoresis system that was operated by Agilent OpenLab CDS 2.7 software. Capillary electrophoresis was performed with a cassette thermostated at 25°C at a constant voltage of 6 kV for anions and −6kV for cations. The small molecules and proteins were detected at 210.0 ± 4.0 nm with a reference wavelength at 500.0 ± 100.0 nm. The capillary was 35 cm in total length and the effective length was 8.5 cm. Each day, the capillary was conditioned by successive flushes of H_2O (30 min) and background electrolyte (BGE) (60 min). Before each run, the capillary was rinsed by flushing BGE (3 min). The analytes were injected into the capillary by vacuum injection at −20 mbar for 4 s, followed by a short plug of BGE at −20 mbar for 2 s.

ACE-MS experiments were performed on an Agilent HP G1600AX 3D-CE system coupled to an Agilent 6340 Ion Trap through a coaxial sheath liquid interface sprayer (Agilent Technologies). The sheath liquid was composed of 5 mM ammonium acetate in methanol/water (80:20, v/v) and was delivered into the sprayer thanks to an Agilent capillary pump (G1376A) at a flow rate of 4.0 µL/min. 6300 Series Trap Control Version 6.2 (Build 62.24) Software was used for data acquisition. The CE and capillary pump were operated by Agilent Chemstation (Rev. B.01.03-SR2 [204]). The MS detection was performed in positive mode using the following ESI-MS conditions: capillary voltage, −3900 V; nebulizer, 2 psi; dry gas, 10.0 L/min; dry temperature, 200°C; skimmer, 40.0 V; capillary exit, 101.2 V; octopole 1 delta classic, 8.00; octopole 2 delta classic, 1.70; trap drive, 25.5; octopole radio frequency, 114.3 Vpp; lens 1, −5.0 V; lens 2, −60.0 V; max accumulation time, 1000.0 ms; ICC target, 500000; scan interval, 119–150 m/z; averages, 2. The analytes were detected as singly charged cations using the following *m/z* values: PABZM – 136.0; lysine – 147.1. Extracted ion electropherograms were smoothed (Gauss, 4.186 s, 2 cycles). The capillary was 60 cm in total and effective length. The capillary was conditioned similarly to CE-UV experiments. β-FXIIa (37.37 µM in 150 mM NMM acetate pH 7.4) was first injected hydrodynamically at 50 mbar for 0, 90, 120, 150, or 180 sec. Then, PABZM (with L-lysine) was inserted at 50 mbar for 8 sec, followed by a short plug of BGE (50 mbar for 2 sec). Capillary electrophoresis was performed with a cassette thermostated at 25°C at a constant voltage of 7 kV.

Sample preparations

The buffer of the FXIIa commercial solution was exchanged with 150 mM NMM acetate pH 7.4 using Amicon® Ultra-0.5 Centrifugal Filter Unit (Merck KGaA, Darmstadt, Germany). Tested compounds were prepared at 20 mM in methanol and kept at −80 °C. Methanol was evaporated at 40°C until dryness using a Centrivap concentrator connected to a cold trap (Labconco, Kansas City, MO). The residue was dissolved in the NMM buffer at the desired concentration. The latter solution was finally 20-fold diluted with water to obtain the injected solution. The concentrations in CE-UV were 40 µM for small molecules and 0.5 mg/mL for proteins. In CE-MS, PABZM, lysine, and FXIIa were injected at 2 µM, 20 µM, and 18.7 µM, respectively.

Data treatment

In CE-UV, the migration times and tailing factors were determined by Agilent OpenLab CDS 2.7 software. In CE-MS, the migration times were obtained thanks to the Agilent DataAnalysis for 6300 Series Ion Trap LC/MS Version 4.0 (Build 234) Software. The corrected migration times of PABZM ($t_{M,corr,PABZM}$) were calculated by applying Eq. 1 (See Supporting Information (SI), Supplemental Data 1). The determination of the K_D was calculated similarly to Nilsson et al.[39] using the corrected migration times (See SI, Supplemental Data 2).

RESULTS AND DISCUSSION

Previously, our team developed direct ACE methods using a diode-array UV detector to validate fragment hits and determine their K_D.[8,9] In the present study, we aimed to adapt the method for hyphenation with MS in order to extend its applicability to compounds with little or no UV−vis absorption and to confirm compound identity during analysis. This additional output helps to avoid false structural assignment of binders, which is a valuable asset during a drug discovery campaign.[2] However, MS detection requires a volatile pH 7.4 buffer and a neutral permanent coating showing minimal adsorption of protein targets and hit compounds. Our previous methods used a Tris-Hepes buffer and a dynamic PEO coating, which are not compatible with MS detectors.

Study design to evaluate the performances of the MS-compatible BGE and coating

For the BGE and coating optimization phase, we selected model compounds (small molecules and proteins) that cover a wide range of physicochemical properties, to select the most universal experimental conditions possible. We employed them to study the phenomenon of adsorption on the inner capillary surface. For small molecules, we used beta-blockers as cationic analytes and non-steroidal anti-inflammatory drugs (NSAIDs) as anionic analytes. Figure 1A shows that the analytes include various lipophilic levels. Indeed, there are anionic and cationic analytes with negative, zero and positive $LogD_{7.4,\ I=0.15M}$ values (Figure 1A). The molecules cover a wide range of MW commonly found in drug-like compounds (Figure 1B).[40] Most molecules have exactly one benzene ring (6 aromatic atom count); but at least one drug in each group has a second aromatic ring (Figure 1B). As shown in Figure 1C, small molecules also exhibit different characteristics in terms of solvent-accessible surface area (ASA). For example, the molecular surface of oxprenolol (orange dot in Figure 1) is predominantly hydrophobic and positive (upper right part of Figure 1C).

For proteins, we selected hard and soft proteins with different MW and charge (Figure 2A). The hard or soft character of a protein is an important concept for understanding protein adsorption at solid-liquid interfaces. Hard proteins retain most of their conformation upon adsorption, while soft proteins are subject to structural changes upon adsorption.[41] Adsorption of hard proteins is governed by electrostatic interactions and dehydration of the sorbent and the protein. On hydrophilic surfaces, hard proteins adsorb only in case of electrostatic attraction. The structural rearrangement of soft proteins adsorbed on solid

surfaces (entropic gain) is an additional driving force that can overcome opposing effects such as electrostatic repulsion and hydrophilic dehydration. [41] Adsorbed proteins typically have 10-40% of their amino acid residues in contact with the solid surface.[41] Thus, a higher MW leads to a greater number of points of attachment to the solid surface. It should be noted that structural stability upon adsorption is difficult to predict. For this study, we only used proteins previously assigned to one of these two categories (Figure 2).[30,41–44] Among the proteins chosen, adalimumab was used as a representative of immunoglobulins G 1 (IgG1), which are soft proteins[44] and the most marketed therapeutic monoclonal antibody.[45] Figures 2B and S1 show the surface properties of the different proteins.

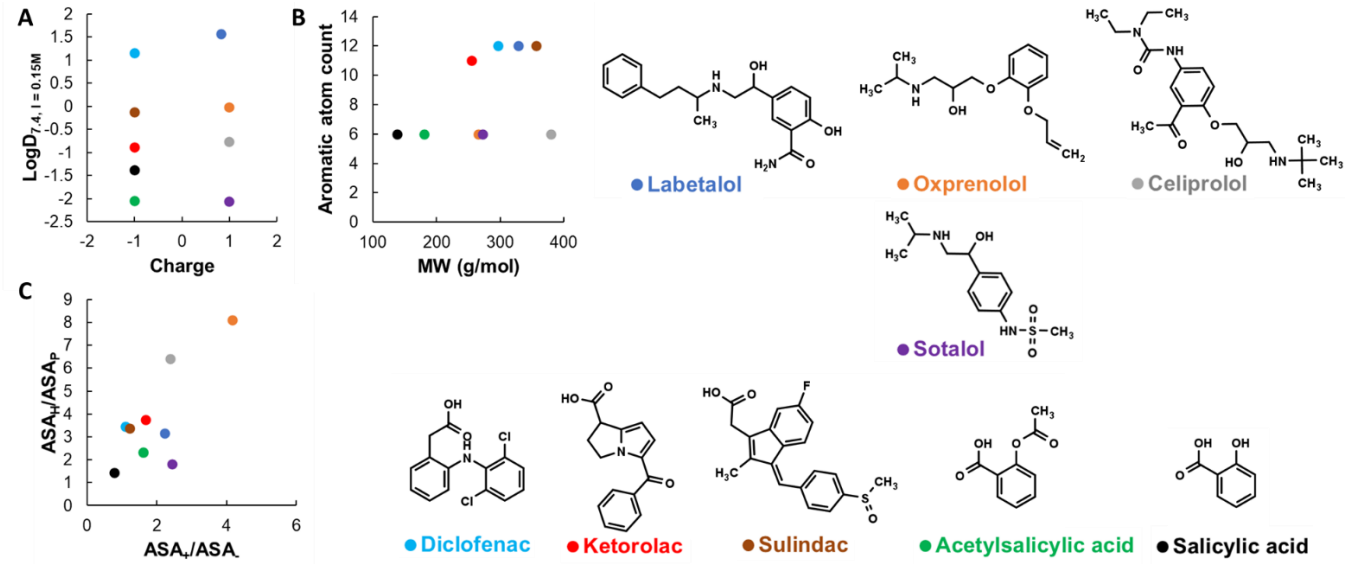

Figure 1. Structure and physicochemical properties of the studied small molecules: charge at pH 7.4 (A, *x*-axis), lipophilicity value at pH 7.4 and ionic strength of 150 mM (A, *y*-axis), molecular weight (B, *x*-axis), number of aromatic atoms (B, *y*-axis), and properties of the molecular surface in terms of charge and hydrophobicity (C). ASA: solvent-accessible surface area at pH 7.4 (solvent radius used = 1.4 Å, approximated radius of a water molecule, Å²) of atoms with a positive partial charge (ASA_+), of atoms with a negative partial charge (ASA_-), of hydrophobic atoms (ASA_H), and of polar atoms (ASA_P), LogD: distribution coefficient, MW: molecular weight.

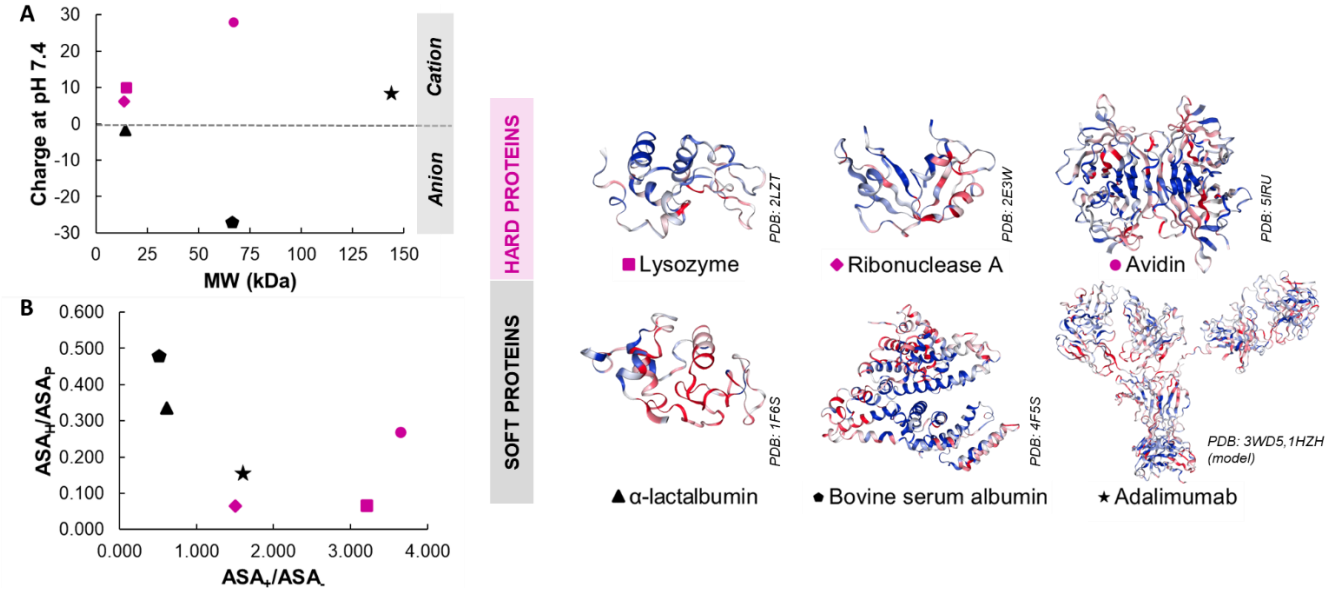

Figure 1. Structure and physicochemical properties of the studied proteins. Panel A shows the charge state at pH 7.4 of the proteins (*y*-axis) and their molecular weight (*x*-axis). Panel B depicts the properties of their molecular surface. The structure of the proteins was depicted using cartoon representation. Red and blue regions are negative and positive patches, respectively. ASA: solvent-accessible surface area at pH 7.4 (solvent radius used = 10 Å, mimicking a flat surface, Å²) of atoms with a positive partial charge (ASA_+), of atoms with a negative partial charge (ASA_-), of hydrophobic atoms (ASA_H), of polar atoms (ASA_P), MW: molecular weight.

Evaluation of *n*-methylmorpholine acetate as BGE

Different concentrations of NMM acetate buffer were compared to the previously used Tris-Hepes buffer.[8–10,46] The measured and calculated characteristics of the buffers are

summarized in Table S1. Increasing NMM concentration led to more viscous BGE with higher background absorbance at 210 nm. We observed cleaner baselines with NMM BGEs (See SI, Figure S2). Compared to Tris-Hepes, 300 mM NMM possessed a lower conductivity despite its higher ionic strength. Moreover, increasing NMM concentration reduced and stabilized the EOF (See SI, Table S1).

Regarding small molecules, we noticed that tailing correlates with the number of H-bond donors (See SI, Figure S3 and Table S3). This correlation was confirmed by testing eight supplemental molecules. Hydrogen bonding was already reported as responsible for the adsorption of numerous small organic molecules on silica surfaces.[47] Ionized silanols that predominantly cover the internal surface of bare-fused silica capillary at pH 7.4 are only H-bond acceptors, which can explain the correlation observed in this study.

As expected[41], in the case of Tris-Hepes, the proteins possessing a molecular surface predominantly positive (Figure 2, ASA_+/ASA_- > 1) strongly interacted with silica (negatively-charged surface at pH 7.4) leading to important peak tailing (lysozyme, ribonuclease A, and adalimumab) or the absence of peak (avidin) (See Figure 3, traces in black). Tailing increased with the MW and the ASA_+/ASA_- ratio. Regarding the soft acidic proteins (α-lactalbumin and BSA), large peaks are observed. Interestingly, peak shape of all the proteins improved with increasing concentration of NMM (See SI, Figures S4 to S9). Using 300 mM or 500 mM NMM, we recorded well-shaped peaks for lysozyme and adalimumab (See Figure 3A and C, respectively), and a peak appeared for avidin (See Figure 3B). This phenomenon can be due to the ability of morpholines to displace adsorbed proteins from silica.[43,48] The desorption property of morpholines is linked to their uncharged form.[48] So, to be efficient, NMM must be used at pH 7.4 or higher. By favorizing protein desorption during CE analysis, proteins spend less time attached to surface. Therefore, tailing is reduced and the soft proteins are less prone to change conformation (which could be linked to the larger peaks observed[43]).[49] Overall, the required NMM concentration to obtain an adequate peak shape correlates with the propensity of the protein to adsorb on silica.

Polydopamine-PIPAAm coating

Although NMM efficiently reduces silica-protein interactions during electromigration, a neutral, antifouling coating is still mandatory to achieve low EOF using an appropriate concentration of NMM. Indeed, a high NMM concentration (500 mM) has an ionic strength around 1.8 times higher than the physiological value (See SI, Table S1) and affects MS detection, causing ion supression.[27] We used a two-levels strategy when studying PDA coatings. First, the coatings had to demonstrate stability over 30 injections in terms of EOF and small molecule migration times. The peak shape of the small molecules was also considered when selecting coatings to prioritize. The second level consisted of evaluating the electromigration of the studied proteins in terms of migration time and peak shape. We compared two PDA deposition and grafting protocols (See Table S2 and Figure S10). The one-pot synthesis was superior to the layer-layer approach since it led to a higher EOF reduction, was stable with a single deposited layer, and required shorter preparation time. The use of 50 mM Tris-HCl had sufficient buffer capacity to support the addition of 25 mg/mL PIPAAm-NH_2. Chemical oxidants (sodium periodate, or copper sulfate with and without hydrogen peroxide) reduced the preparation time, but did not lead to stable coatings. To reduce the tailing observed with diclofenac, sulindac, celiprolol, and labetalol (See SI, Figure S11), several endcapping strategies were investigated. Our best results were obtained with the Tris endcapping. We also observed that PDA-coated capillaries must be kept in water in order to avoid crack formation in the PDA layer (See SI, Figure S12). [50] Conversely, air flushes altered the migration times of small molecules.

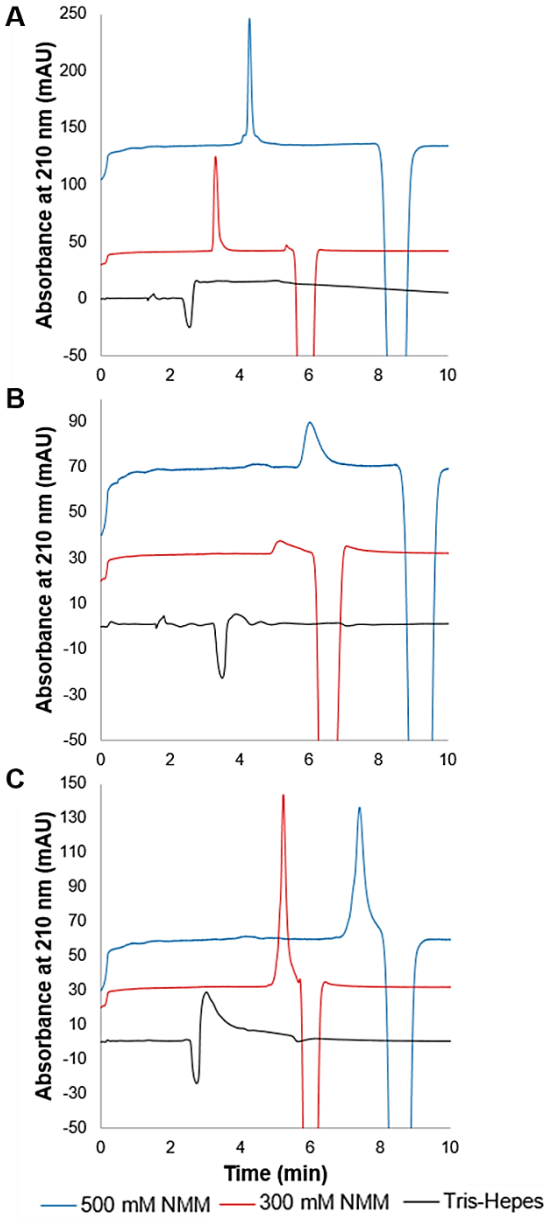

Figure 3. Electropherograms of lysozyme (A), avidin (B), and adalimumab (C) with different BGE on bare-fused silica capillary. The negative peaks are waterdips due to the sample matrix (BGE 10-fold diluted with water) and correspond to the magnitude of the EOF. (A) Highly distorted peak of lysozyme detected after the EOF was observed with Tris-Hepes. Tailing was still present with the 300 mM NMM BGE. 500 mM NMM generated a well-shaped main peak with two additional species at its base. (B) No

peak was detected with Tris-Hepes. A distorted peak (end of the tailing after the EOF) appeared with the 300 mM NMM BGE. 500 mM NMM generated a peak with slight tailing. (C) A distorted peak was detected with Tris-Hepes. 300 mM NMM and 500 mM NMM BGEs generated a well-shaped main peak. Two additional species were separated with the 500 mM NMM BGE. BGE: background electrolytes, EOF: electro-osmotic flow.

Interestingly, we observed that the small molecules with the highest tailing factors (TF) had a second aromatic ring. Thus, we suspected a major contribution of π–π stacking and cation–π interactions with the PDA layer. These interactions maintain non-covalent complexes in the PDA layer.[51] Therefore, additional NSAIDs and beta-blockers were tested to expand the dataset. Two pairs of compounds possessing similar properties in terms of charge and lipophilic character but with different expected strength of π stacking interactions (propranolol:betaxolol and flurbiprofen:ibuprofen) were investigated. The molecules bearing a moiety that forms strong π stacking interactions, such as naphthalene[52] (propranolol, TF = 7.84 ± 0.45) and biphenyl[53] (flurbiprofen, TF = 7.92 ± 0.29), showed highly distorted peaks compared to those with a single phenyl group (betaxolol: TF = 2.68 ± 0.26 and ibuprofen: TF = 1.36 ± 0.04, respectively). The cyclopropyl group of betaxolol (TF = 2.68 ± 0.26) also altered the peak shape (vs metoprolol, TF = 1.56 ± 0.02) (See SI, Table S3). Cyclopropane possesses uncommon C−C single bonds that are closer to C=C double bonds in terms of properties. Therefore, this moiety can form CH−π interactions.[54] These differences in tailing factor were not observed on bare-fused silica capillaries (See SI, Table S3).

For proteins, an adequate peak shape for all the tested proteins was obtained with 300 mM NMM BGE using our best PDA-PIPAAm capillary (See Figure 4). 150 mM NMM BGE was also tested, showing satisfactory results for both slightly basic and acidic proteins. Strongly basic proteins and antibodies required 300 mM NMM BGE. Overall, the combination of NMM and the neutral coating allowed us to obtain better results compared to other studies.[55–57] Indeed, previous analyzes of proteins on different neutral-coated capillary have reported drastic peak distortion at pH 7.[55–57] Most papers[58–61] performed protein analysis in strong acidic conditions (pH 2-3.5).

Binding measurements using CE-MS

To investigate the potential of our method to measure interactions under near-physiological conditions, we monitored PABZM, a known β-FXIIa ligand. 150 mM NMM BGE was sufficient to provide an adequate peak shape for both PABZM and β-FXIIa, an acidic protein (pI = 4.7-4.9[62,63]) of 30 kDa. The voltage was set at the maximal value (7 kV) that generated less than 50 µA (MS compatibility) and an adequate heat dissipation (See SI, Figure S13). Under these conditions, we did not observe any polymer leakage in the MS instrument. It should be noted that to reduce the MS background, contamination of NMM by *n*-methylmorpholin N-oxide should be limited by using highly pure NMM and storing it under inert atmosphere at 4°C (See SI, Supplemental Data 3).

Concerning the determination of the K_D, we customized the approach of Nilsson et al.[39] that determines the affinity directly from migration times. This only requires prior knowledge of the amount of protein loaded, the effective length of the capillary, and the internal radius of the capillary. Since the thickness of PDA films reaches a maximum 45 nm[64], it was considered negligible. In CE-MS, it is common to observe variability in migration times due to the coupling interface. To alleviate this restriction, we introduced a non-interacting analyte (L- lysine) preferred over a flow marker because the EOF is very low. The corrected migration times ($t_{M,corr}$) of PABZM in min were calculated according to Eq. 1 (See SI, Supplemental Data 1).

$$t_{M,corr} = \frac{1}{\left(\frac{1}{t_{M,obs}} - \frac{1}{t_{M,obs,lys}} + \frac{\mu_{eff,lys}}{a}\right)} \qquad (Eq.\,1)$$

where $\frac{\mu_{eff,lys}}{a}$ had a value of 0.024 min^{-1}.

The calculated K_D of PABZM-FXIIa interaction by CE-MS was 153.9 [149.2-158.9] µM (See Figure 5 and SI, Figure S14). This value is similar to its inhibition constant (K_i) previously reported at 163.2 [162.2-164.2] µM.[8,10] The potency ratio between these two values is 1.06, which is considered as not significantly different in FXIIa medicinal chemistry program.[10]

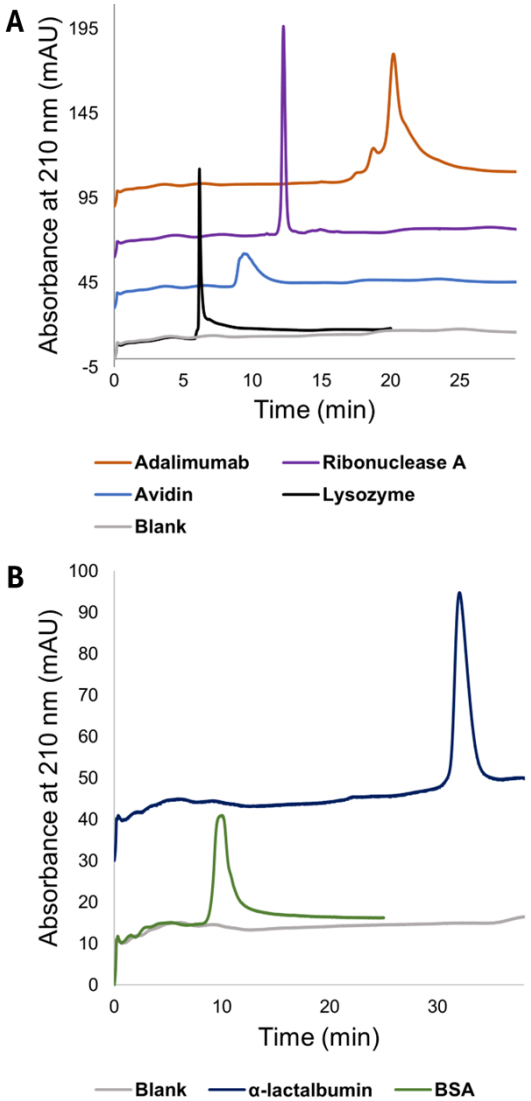

Figure 4. Electropherograms of the studied basic (A) and acidic (B) proteins on the best PDA-PIPAAm coated capillary. BSA: bovine serum albumin, PIPAAm: poly(N-isopropylacrylamide), PDA: polydopamine.

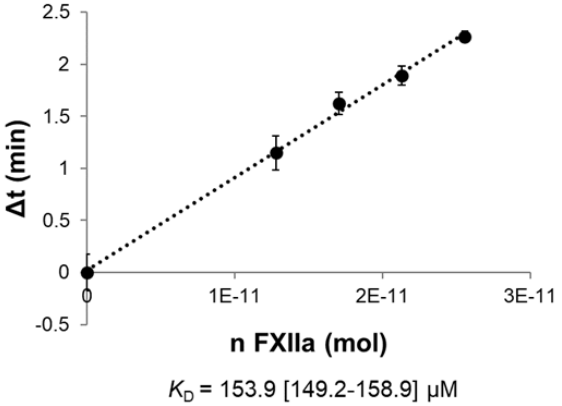

Figure 5. Determination of the dissociation constant (K_D) of PABZM by ACE-MS: plot of the difference in corrected migration times (Δt, in min) against the amount of injected β-FXIIa (n, in mol). FXIIa: coagulation factor XIIa, and PABZM: *p*-aminobenzamidine.

CONCLUSION

Protein adsorption in capillary electrophoresis is a common issue. The adhesion of protein on the silica surface is known to deteriorate the repeatability of EOF and migration times, peak shape, and resolution.[65] Being able to desorb proteins from the capillary surface typically requires harsh treatments, such as flushing the capillary with 2M HCl or 85% m/m phosphoric acid.[66] Several coatings, including PVA and PDA, are incompatible with these strong acidic conditions. NMM addresses this unmet need by desorbing proteins in a gentler way (pH 7.4, aqueous solution). Besides its desorption property, NMM is an interesting buffering component for capillary electrophoresis because of its low conductivity and MS compatibility.

We showed that one-pot PDA deposition is an efficient strategy to generate MS-compatible coating that is stable at physiological pH. Stable coatings at neutral pH are sparse. The most common strategy to covalently attach the desired polymer on silica is through siloxane linkages. However, these bonds are already damaged at pH superior to 4.6.[19] PVA is stable at 7.4; but it does not support modulations. On the contrary, PDA can immobilize polymers of diverse properties.[56,59–61,67,68] However, the PDA layer is not an inert surface and interacts with small molecules through π interactions, which can be attenuated by endcapping PDA with Tris.

We showed that the combination of NMM-based BGE and PDA-based coating enables the successful hyphenation of ACE with MS in physiological conditions. Ligand-protein interaction studies by ACE-MS require low amount of tested compound and protein per experiment. Compared to our ACE-UV approach, the ACE-MS can detect a low UV−vis absorbent compounds (such as L-lysine, in the present application) and be performed at lower concentration of analyte. However, a non-interacting analyte is mandatory to monitor the liquid flow in each experiment and, in consequence, correct the migration times.

ASSOCIATED CONTENT

Supporting Information

The Supporting Information is available free of charge on the ACS Publications website.

Physicochemical properties of the studied BGE, full mathematical developments, remark on the use of NMM for MS, additional data, including electropherograms, properties of the proteins' surface, representation of the coatings' protocols, Ohm's law plot, and tailing factors of the small molecules on bare-fused silica and PDA-PIPAAm coated capillaries. (PDF)

Computed physicochemical properties of small molecules. (XLSX)

Physicochemical properties of proteins. (XLSX)

AUTHOR INFORMATION

Corresponding Author

* E-mail address: marianne.fillet@uliege.be

Author Contributions

The manuscript was written through contributions of all authors.

ACKNOWLEDGMENT

C. D. received funding from the National Fund for Scientific Research (FNRS) [grant number 40017636]; and Fondation Léon Frédéricq [grant number 2020-2021-30-C.F.F]. M. F. received funding from the University of Liège Fonds Spéciaux, Crédits facultaires [grant number 14758].

REFERENCES

(1) Kairys, V.; Baranauskiene, L.; Kazlauskiene, M.; Matulis, D.; Kazlauskas, E. Binding Affinity in Drug Design: Experimental and Computational Techniques. *Expert Opin. Drug Discov.* **2019**, *14* (8), 755–768.

(2) Jones, P.; McElroy, S.; Morrison, A.; Pannifer, A. The Importance of Triaging in Determining the Quality of Output from High-Throughput Screening. *Future Med. Chem.* **2015**, *7* (14), 1847–1852.

(3) Copeland, R. A. *Evaluation of Enzyme Inhibitors in Drug Discovery : A Guide for Medicinal Chemists and Pharmacologists*, Second Edi.; John Wiley & Sons: Hoboken, New Jersey, 2013.

(4) Paul, S. M.; Mytelka, D. S.; Dunwiddie, C. T.; Persinger, C. C.; Munos, B. H.; Lindborg, S. R.; Schacht, A. L. How to Improve R&D Productivity: The Pharmaceutical Industry's Grand Challenge. *Nat. Rev. Drug Discov.* **2010**, *9* (3), 203–214.

(5) Renaud, J. P.; Chung, C. W.; Danielson, U. H.; Egner, U.; Hennig, M.; Hubbard, R. E.; Nar, H. Biophysics in Drug Discovery: Impact, Challenges and Opportunities. *Nat. Rev. Drug Discov.* **2016**, *15* (10), 679–698.

(6) Mironov, G. G.; Logie, J.; Okhonin, V.; Renaud, J. B.; Mayer, P. M.; Berezovski, M. V. Comparative Study of Three Methods for Affinity Measurements: Capillary Electrophoresis Coupled with UV Detection and Mass Spectrometry, and Direct Infusion Mass Spectrometry. *J. Am. Soc. Mass Spectrom.* **2012**, *23* (7), 1232–1240.

(7) Davoine, C.; Pochet, L.; Fillet, M. Advances in Analytical Technologies Detecting and Characterizing Noncovalent Interactions for Fragment-Based Drug Discovery. *TrAC Trends Anal. Chem.* **2023**, *166*, 117161.

(8) Davoine, C.; Fillet, M.; Pochet, L. Capillary Electrophoresis as a Fragment Screening Tool to Cross-Validate Hits from Chromogenic Assay: Application to FXIIa. *Talanta* **2021**, *226*, 122163.

(9) Farcaş, E.; Bouckaert, C.; Servais, A. C.; Hanson, J.; Pochet, L.; Fillet, M. Partial Filling Affinity Capillary Electrophoresis as a Useful Tool for Fragment-Based Drug Discovery: A Proof of Concept on Thrombin. *Anal. Chim. Acta* **2017**, *984*, 211–222.

(10) Davoine, C.; Pardo, A.; Pochet, L.; Fillet, M. Fragment Hit Discovery and Binding Site Characterization by Indirect Affinity

Capillary Electrophoresis: Application to Factor XIIa. *Anal. Chem.* **2021**, *93* (44), 14802–14809.

(11) Dubský, P.; Dvořák, M.; Ansorge, M. Affinity Capillary Electrophoresis: The Theory of Electromigration. *Anal. Bioanal. Chem.* **2016**, *408* (30), 8623–8641.

(12) Olabi, M.; Stein, M.; Wätzig, H. Affinity Capillary Electrophoresis for Studying Interactions in Life Sciences. *Methods* **2018**, *146* (May), 76–92.

(13) Chu, Y.-H.; Dunayevskiy, Y. M.; Kirby, D. P.; Vouros, P.; Karger, B. L. Affinity Capillary Electrophoresis−Mass Spectrometry for Screening Combinatorial Libraries. *J. Am. Chem. Soc.* **1996**, *118* (33), 7827–7835.

(14) Dunayevskiy, Y. M.; Lyubarskaya, Y. V.; Chu, Y.-H.; Vouros, P.; Karger, B. L. Simultaneous Measurement of Nineteen Binding Constants of Peptides to Vancomycin Using Affinity Capillary Electrophoresis−Mass Spectrometry. *J. Med. Chem.* **1998**, *41* (7), 1201–1204.

(15) Lynen, F.; Zhao, Y.; Becu, C.; Borremans, F.; Sandra, P. Considerations Concerning Interaction Characterization of Oligopeptide Mixtures with Vancomycin Using Affinity Capillary Electrophoresis-Electrospray Mass Spectrometry. *Electrophoresis* **1999**, *20* (12), 2462–2474.

(16) Gstöttner, C.; Hook, M.; Christopeit, T.; Knaupp, A.; Schlothauer, T.; Reusch, D.; Haberger, M.; Wuhrer, M.; Domínguez-Vega, E. Affinity Capillary Electrophoresis–Mass Spectrometry as a Tool to Unravel Proteoform-Specific Antibody–Receptor Interactions. *Anal. Chem.* **2021**, *93* (45), 15133–15141.

(17) Gstöttner, C.; Knaupp, A.; Vidarsson, G.; Reusch, D.; Schlothauer, T.; Wuhrer, M.; Domínguez-Vega, E. Affinity Capillary Electrophoresis – Mass Spectrometry Permits Direct Binding Assessment of IgG and FcγRIIa in a Glycoform-Resolved Manner. *Front. Immunol.* **2022**, *13*.

(18) Zhu, G.; Sun, L.; Dovichi, N. J. Thermally-Initiated Free Radical Polymerization for Reproducible Production of Stable Linear Polyacrylamide Coated Capillaries, and Their Application to Proteomic Analysis Using Capillary Zone Electrophoresis–Mass Spectrometry. *Talanta* **2016**, *146*, 839–843.

(19) Horvath, J.; Dolník, V. Polymer Wall Coatings for Capillary Electrophoresis. *Electrophoresis* **2001**, *22* (4), 644–655.

(20) Zhang, H.; Yang, F. Applications of Polydopamine Modifications in Capillary Electrophoretic Analysis. *J. Sep. Sci.* **2019**, *42* (1), 342–359.

(21) Ryu, J. H.; Messersmith, P. B.; Lee, H. Polydopamine Surface Chemistry: A Decade of Discovery. *ACS Appl. Mater. Interfaces* **2018**, *10* (9), 7523–7540.

(22) Wei, H.; Ren, J.; Han, B.; Xu, L.; Han, L.; Jia, L. Stability of Polydopamine and Poly(DOPA) Melanin-like Films on the Surface of Polymer Membranes under Strongly Acidic and Alkaline Conditions. *Colloids Surfaces B Biointerfaces* **2013**, *110*, 22–28.

(23) Hemmatpour, H.; De Luca, O.; Crestani, D.; Stuart, M. C. A.; Lasorsa, A.; van der Wel, P. C. A.; Loos, K.; Giousis, T.; Haddadi-Asl, V.; Rudolf, P. New Insights in Polydopamine Formation via Surface Adsorption. *Nat. Commun.* **2023**, *14* (1), 664.

(24) Du, H.; Zhang, C.; Mao, K.; Wang, Y. A Star-Shaped Poly(2-Methyl-2-Oxazoline)-Based Antifouling Coating: Application in Investigation of the Interaction between Acetaminophen and Bovine Serum Albumin by Frontal Analysis Capillary Electrophoresis. *Talanta* **2017**, *170*, 275–285.

(25) Hedges, J. B.; Vahidi, S.; Yue, X.; Konermann, L. Effects of Ammonium Bicarbonate on the Electrospray Mass Spectra of Proteins: Evidence for Bubble-Induced Unfolding. *Anal. Chem.* **2013**, *85* (13), 6469–6476.

(26) Settimo, L.; Bellman, K.; Knegtel, R. M. A. Comparison of the Accuracy of Experimental and Predicted PKa Values of Basic and Acidic Compounds. *Pharm. Res.* **2014**, *31* (4), 1082–1095.

(27) Catai, J. R.; Toraño, J. S.; de Jong, G. J.; Somsen, G. W. Capillary Electrophoresis–Mass Spectrometry of Proteins at Medium PH Using Bilayer-Coated Capillaries. *Analyst* **2007**, *132* (1), 75–81.

(28) Witzel, M. T.; Veltri, L. M.; Kostelic, M.; Elshamy, Y. S.; Lucas, J. A.; Lai, S.; Du, C.; Wysocki, V. H.; Holland, L. A. Protein Analysis Using Capillary Electrophoresis Coupled to Mass Spectrometry through Vibrating Sharp-edge Spray Ionization. *Electrophoresis* **2024**, *45* (17–18), 1597–1605.

(29) Dovhunová, M.; Malý, M.; Dubský, P.; Gerlero, G. S.; Kler, P. A. Generalized Model of the Linear Theory of Electromigration and Its Application to Electrokinetic Chromatography: Capillary Zone Electrophoretic Systems with Complex-Forming Equilibria. *J. Chromatogr. A* **2020**, *1610*, 460595.

(30) Shirahama, H.; Lyklema, J.; Norde, W. Comparative Protein Adsorption in Model Systems. *J. Colloid Interface Sci.* **1990**, *139* (1), 177–187.

(31) Nau, F.; Guérin-Dubiard, C.; Croguennec, T. Avidin. In *Bioactive Egg Compounds*; Springer Berlin Heidelberg: Berlin, Heidelberg, 2007; pp 75–80.

(32) Zhang, F.; Weggler, S.; Ziller, M. J.; Ianeselli, L.; Heck, B. S.; Hildebrandt, A.; Kohlbacher, O.; Skoda, M. W. A.; Jacobs, R. M. J.; Schreiber, F. Universality of Protein Reentrant Condensation in Solution Induced by Multivalent Metal Ions. *Proteins Struct. Funct. Bioinforma.* **2010**, *78* (16), 3450–3457.

(33) Füssl, F.; Trappe, A.; Cook, K.; Scheffler, K.; Fitzgerald, O.; Bones, J. Comprehensive Characterisation of the Heterogeneity of Adalimumab via Charge Variant Analysis Hyphenated On-Line to Native High Resolution Orbitrap Mass Spectrometry. *MAbs* **2019**, *11* (1), 116–128.

(34) Hebditch, M.; Warwicker, J. Protein-Sol PKa: Prediction of Electrostatic Frustration, with Application to Coronaviruses. *Bioinformatics* **2020**, *36* (20), 5112–5114.

(35) Saporiti, S.; Parravicini, C.; Pergola, C.; Guerrini, U.; Rossi, M.; Centola, F.; Eberini, I. IgG1 Conformational Behavior: Elucidation of the N-Glycosylation Role via Molecular Dynamics. *Biophys. J.* **2021**, *120* (23), 5355–5370.

(36) Fraczkiewicz, R.; Braun, W. Exact and Efficient Analytical Calculation of the Accessible Surface Areas and Their Gradients for Macromolecules. *J. Comput. Chem.* **1998**, *19* (3), 319–333.

(37) Nicolau, D. V.; Paszek, E.; Fulga, F.; Nicolau, D. V. Protein Molecular Surface Mapped at Different Geometrical Resolutions. *PLoS One* **2013**, *8* (3), e58896.

(38) Hebditch, M.; Warwicker, J. Web-Based Display of Protein Surface and PH-Dependent Properties for Assessing the Developability of Biotherapeutics. *Sci. Rep.* **2019**, *9* (1), 1969.

(39) Nilsson, M.; Harang, V.; Bergström, M.; Ohlson, S.; Isaksson, R.; Johansson, G. Determination of Protein-Ligand Affinity Constants from Direct Migration Time in Capillary Electrophoresis. *Electrophoresis* **2004**, *25* (12), 1829–1836.

(40) Yusof, I.; Segall, M. D. Considering the Impact Drug-like Properties Have on the Chance of Success. *Drug Discov. Today* **2013**, *18* (13–14), 659–666.

(41) Norde, W. Adsorption of Proteins at Solid-Liquid Interfaces. *Cells Mater.* **1995**, *5* (1), 97–112.

(42) Coglitore, D.; Janot, J.-M.; Balme, S. Protein at Liquid Solid Interfaces: Toward a New Paradigm to Change the Approach to Design Hybrid Protein/Solid-State Materials. *Adv. Colloid Interface Sci.* **2019**, *270*, 278–292.

(43) Norde, W.; Anusiem, A. C. I. Adsorption, Desorption and Re-Adsorption of Proteins on Solid Surfaces. *Colloids and Surfaces* **1992**, *66* (1), 73–80.

(44) Chen, X.; Chen, J.; Huang, N. The Structure, Formation, and Effect of Plasma Protein Layer on the Blood Contact Materials: A Review. *Biosurface and Biotribology* **2022**, *8* (1), 1–14.

(45) Alejandra, W.-P.; Miriam Irene, J.-P.; Fabio Antonio, G.-S.; Patricia, R.-G. R.; Elizabeth, T.-A.; Aleman-Aguilar, J. P.; Rebeca, G.-V. Production of Monoclonal Antibodies for Therapeutic Purposes: A Review. *Int. Immunopharmacol.* **2023**, *120*, 110376.

(46) Farcaş, E.; Hanson, J.; Pochet, L.; Fillet, M. Capillary Electrophoretic Mobility Shift Displacement Assay for the Assessment of Weak Drug-Protein Interactions. *Anal. Chim. Acta* **2018**, *1034*, 214–222.

(47) Parida, S. K.; Dash, S.; Patel, S.; Mishra, B. K. Adsorption of Organic Molecules on Silica Surface. *Adv. Colloid Interface Sci.* **2006**, *121* (1–3), 77–110.

(48) Norde, W.; MacRitchie, F.; Nowicka, G.; Lyklema, J. Protein Adsorption at Solid-Liquid Interfaces: Reversibility and Conformation Aspects. *J. Colloid Interface Sci.* **1986**, *112* (2), 447–456.
(49) Rabe, M.; Verdes, D.; Seeger, S. Understanding Protein Adsorption Phenomena at Solid Surfaces. *Adv. Colloid Interface Sci.* **2011**, *162* (1–2), 87–106.
(50) Goh, S. C.; Luan, Y.; Wang, X.; Du, H.; Chau, C.; Schellhorn, H. E.; Brash, J. L.; Chen, H.; Fang, Q. Polydopamine–Polyethylene Glycol–Albumin Antifouling Coatings on Multiple Substrates. *J. Mater. Chem. B* **2018**, *6* (6), 940–949.
(51) Hong, S.; Na, Y. S.; Choi, S.; Song, I. T.; Kim, W. Y.; Lee, H. Non-Covalent Self-Assembly and Covalent Polymerization Co-Contribute to Polydopamine Formation. *Adv. Funct. Mater.* **2012**, *22* (22), 4711–4717.
(52) Makar, S.; Saha, T.; Singh, S. K. Naphthalene, a Versatile Platform in Medicinal Chemistry: Sky-High Perspective. *Eur. J. Med. Chem.* **2019**, *161*, 252–276.
(53) Singh, S.; Geetha, P.; Ramajayam, R. Isolation, Synthesis and Medicinal Chemistry of Biphenyl Analogs – A Review. *Results Chem.* **2023**, *6*, 101135.
(54) Talele, T. T. The "Cyclopropyl Fragment" Is a Versatile Player That Frequently Appears in Preclinical/Clinical Drug Molecules. *J. Med. Chem.* **2016**, *59* (19), 8712–8756.
(55) Bruin, G. J. M.; Chang, J. P.; Kuhlman, R. H.; Zegers, K.; Kraak, J. C.; Poppe, H. Capillary Zone Electrophoretic Separations of Proteins in Polyethylene Glycol-Modified Capillaries. *J. Chromatogr. A* **1989**, *471*, 429–436.
(56) Zeng, R.; Luo, Z.; Zhou, D.; Cao, F.; Wang, Y. A Novel PEG Coating Immobilized onto Capillary through Polydopamine Coating for Separation of Proteins in CE. *Electrophoresis* **2010**, *31* (19), 3334–3341.
(57) Schmalzing, D.; Piggee, C. A.; Foret, F.; Carrilho, E.; Karger, B. L. Characterization and Performance of a Neutral Hydrophilic Coating for the Capillary Electrophoretic Separation of Biopolymers. *J. Chromatogr. A* **1993**, *652* (1), 149–159.
(58) Chen, L.; Zhang, Y.; Tan, L.; Liu, S.; Wang, Y. Assembly of Poly(Dopamine)/Poly(Acrylamide) Mixed Coatings by a Single-Step Surface Modification Strategy and Its Application to the Separation of Proteins Using Capillary Electrophoresis. *J. Sep. Sci.* **2015**, *38* (16), 2915–2923.
(59) Chen, L.; Liu, G.; Liu, S.; Bai, L.; Wang, Y. Preparation and Characterization of Brush-like PEGMA-Graft-PDA Coating and Its Application for Protein Separation by CE. *J. Biomater. Sci. Polym. Ed.* **2014**, *25* (12), 1306–1327.
(60) Yan, Y. H.; Atif, M.; Liu, R. Y.; Zhu, H. K.; Chen, L. J. Design of Comb-like Poly(2-Methyl-2-Oxazoline) and Its Rapid Co-Deposition with Dopamine for the Study of Antifouling Properties. *J. Biomater. Sci. Polym. Ed.* **2020**, *31* (4), 423–438.
(61) Chen, L.; Tan, L.; Liu, S.; Bai, L.; Wang, Y. Surface Modification by Grafting of Poly(SBMA-Co-AEMA)-g-PDA Coating and Its Application in CE. *J. Biomater. Sci. Polym. Ed.* **2014**, *25* (8), 766–785.
(62) Davoine, C.; Bouckaert, C.; Fillet, M.; Pochet, L. Factor XII/XIIa Inhibitors: Their Discovery, Development, and Potential Indications. *Eur. J. Med. Chem.* **2020**, *208*, 112753.
(63) Papageorgiou, P. C.; Pourdjabbar, A.; Amfilochiadis, A. A.; Diamandis, E. P.; Boomsma, F.; Osmond, D. H. Are Cardiovascular and Sympathoadrenal Effects of Human "New Pressor Protein" Preparations Attributable to Human Coagulation β-FXIIa? *Am. J. Physiol. Circ. Physiol.* **2004**, *286* (3), H837–H846.
(64) Della Vecchia, N. F.; Luchini, A.; Napolitano, A.; D'Errico, G.; Vitiello, G.; Szekely, N.; D'Ischia, M.; Paduano, L. Tris Buffer Modulates Polydopamine Growth, Aggregation, and Paramagnetic Properties. *Langmuir* **2014**, *30* (32), 9811–9818.
(65) Stutz, H. Protein Attachment onto Silica Surfaces - A Survey of Molecular Fundamentals, Resulting Effects and Novel Preventive Strategies in CE. *Electrophoresis* **2009**, *30* (12), 2032–2061.
(66) Suratman, A.; Wätzig, H. Reproducible Protein Analysis by CE Using Linear Polyacrylamide-Coated Capillaries and Hydrochloric Acid Rinsing. *Electrophoresis* **2007**, *28* (13), 2324–2328.
(67) Long, W.; You, M.; Li, J.; Wang, Y.; Wang, D.; Tao, X.; Rao, L.; Xia, Z.; Fu, Q. Sulfonic Functionalized Polydopamine Coatings with PH-Independent Surface Charge for Optimizing Capillary Electrophoretic Separations. *Molecules* **2024**, *29* (7).
(68) Fu, Q.; Li, X.; Zhang, Q.; Yang, F.; Wei, W.; Xia, Z. A Facile and Versatile Approach for Controlling Electroosmotic Flow in Capillary Electrophoresis via Mussel Inspired Polydopamine/Polyethyleneimine Co-Deposition. *J. Chromatogr. A* **2015**, *1416*, 94–102.

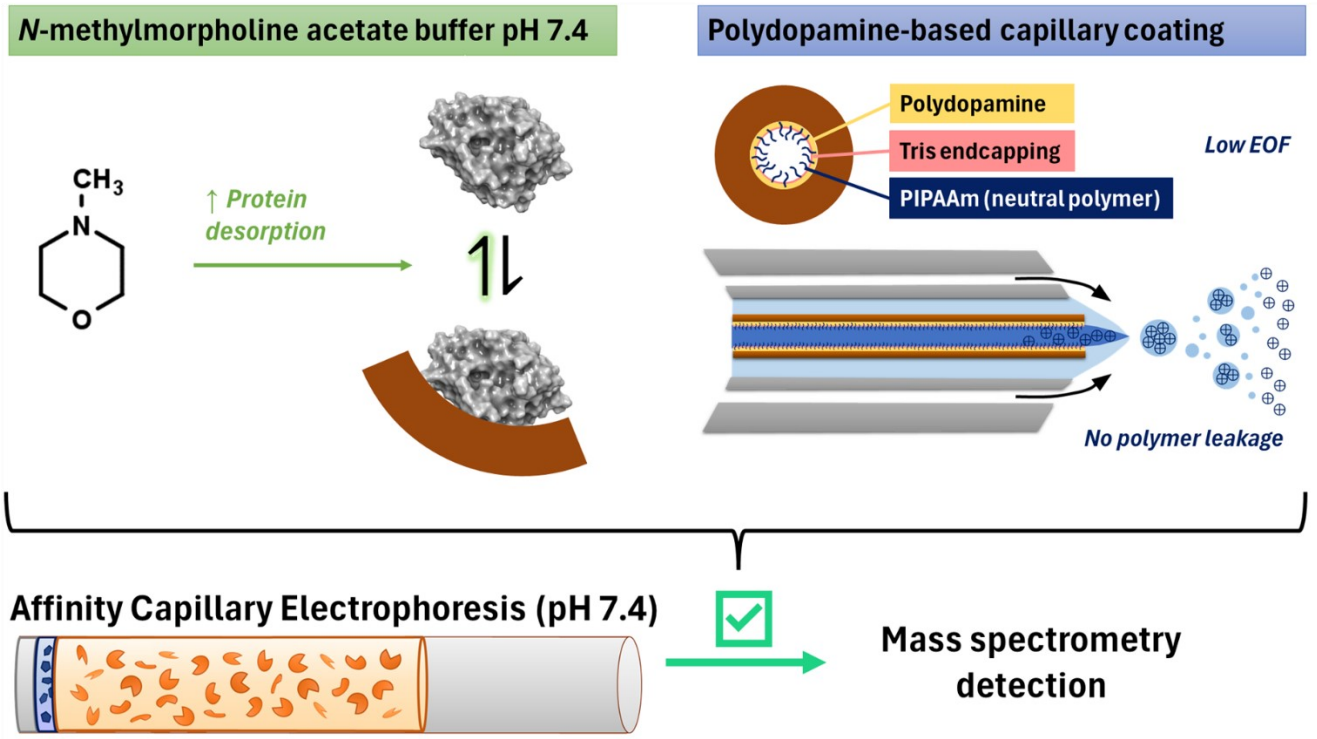
N-methylmorpholine acetate buffer pH 7.4
CH3
N
O
↑ Protein desorption
Polydopamine-based capillary coating
Polydopamine
Tris endcapping
PIPAAm (neutral polymer)
Low EOF
No polymer leakage
Affinity Capillary Electrophoresis (pH 7.4)
Mass spectrometry detection